ICARUS **120,** 140–157 (1996)
ARTICLE NO. 0042

Erosion and Ejecta Reaccretion on 243 Ida and Its Moon

PAUL GEISSLER, JEAN-MARC PETIT,[1] DANIEL D. DURDA, RICHARD GREENBERG, WILLIAM BOTTKE, AND MICHAEL NOLAN[2]

Lunar and Planetary Laboratory, University of Arizona, Tucson, Arizona 85721
E-mail: geissler@pirl.lpl.arizona.edu

AND

JEFFREY MOORE

NASA Ames Research Center, Moffett Field, California 94035

Received April 3, 1995; revised July 31, 1995

Galileo images of Asteroid 243 Ida and its satellite Dactyl show surfaces which are dominantly shaped by impact cratering. A number of observations suggest that ejecta from hypervelocity impacts on Ida can be distributed far and wide across the Ida system, following trajectories substantially affected by the low gravity, nonspherical shape, and rapid rotation of the asteroid. We explore the processes of reaccretion and escape of ejecta on Ida and Dactyl using three-dimensional numerical simulations which allow us to compare the theoretical effects of orbital dynamics with observations of surface morphology.

The effects of rotation, launch location, and initial launch speed are first examined for the case of an ideal triaxial ellipsoid with Ida's approximate shape and density. Ejecta launched at low speeds ($V \ll V_{esc}$) reimpact near the source craters, forming well-defined ejecta blankets which are asymmetric in morphology between leading and trailing rotational surfaces. The net effect of cratering at low ejecta launch velocities is to produce a thick regolith which is evenly distributed across the surface of the asteroid. In contrast, no clearly defined ejecta blankets are formed when ejecta is launched at higher initial velocities ($V \sim V_{esc}$). Most of the ejecta escapes, while that which is retained is preferentially derived from the rotational trailing surfaces. These particles spend a significant time in temporary orbit around the asteroid, in comparison to the asteroid's rotation period, and tend to be swept up onto rotational leading surfaces upon reimpact. The net effect of impact cratering with high ejecta launch velocities is to produce a thinner and less uniform soil cover, with concentrations on the asteroids' rotational leading surfaces.

Using a realistic model for the shape of Ida (P. Thomas, J. Veverka, B. Carcich, M. J. S. Belton, R. Sullivan, and M. Davies 1996, *Icarus* 120, 000–000), we find that an extensive color/albedo unit which dominates the northern and western hemispheres of the asteroid can be explained as the result of reaccretion of impact ejecta from the large and evidently recent crater "Azzurra." Initial ejection speeds required to match the color observations are on the order of a few meters per second, consistent with models (e.g., M. C. Nolan, E. Asphaug, H. J. Melosh, and R. Greenberg 1996, *Icarus,* submitted; E. Asphaug, J. Moore, D. Morrison, W. Benz, and R. Sullivan 1996, *Icarus* 120, 158–184) that multikilometer craters on Ida form in the gravity-dominated regime and are net producers of locally retained regolith. Azzurra ejecta launched in the direction of rotation at speeds near 10 m/sec are lofted over the asteroid and swept up onto the rotational leading surface on the opposite side. The landing locations of these particles closely match the distribution of large ejecta blocks observed in high resolution images of Ida (P. Lee, J. Veverka, P. Thomas, P. Helfstein, M. J. S. Belton, C. Chapman, R. Greeley, R. Pappalardo, R. Sullivan, and J. W. Head 1996, *Icarus* 120, 87–105).

Ida's shape and rotation allow escape of ejecta launched at speeds far below the escape velocity of a nonrotating sphere of Ida's volume and presumed density. While little ejecta from Ida is captured by Dactyl, about half of the mass ejected from Dactyl at speeds of up to 20 m/sec eventually falls on Ida. Particles launched at speeds just barely exceeding Dactyl's escape velocity can enter relatively long-term orbit around Ida, but few are ultimately reaccreted by the satellite. Because of its low gravity, erosion of Dactyl would take place on exceedingly short time scales if unconsolidated materials compose the satellite and crater formation is in the gravity regime. If Dactyl is a solid rock, then its shape has evolved from a presumably irregular initial fragment to its present remarkably rounded figure by collision with a population of impactors too small to be detected by counting visible craters. As the smallest solar

[1] Permanent address: Observatoire de Nice, B.P. 229 06304, Nice Cedex 4, France.

[2] Permanent address: Arecibo Observatory, P.O. Box 995, Arecibo, Puerto Rico 00613.

0019-1035/96 $18.00

system object yet imaged by a spacecraft, the morphology of Dactyl is an important clue to the asteroid population at the smallest sizes.

1. INTRODUCTION

The discovery of large ejecta blocks distributed nonuniformly across the surface of Asteroid 243 Ida (Belton *et al.* 1994) presents something of a puzzle. Because of their size—ranging from 150 m down to the limit of resolution (about 40 m)—ejecta blocks are susceptible to catastrophic disruption on comparatively short time scales by collision of meter-sized projectiles which are far more numerous than those responsible for the larger impact events that formed the blocks. Hence, these ''boulders'' are probably among the youngest features of Ida's surface. The blocks visible on the portion of Ida seen at high resolution (about 30% of the surface) have a distinctly nonuniform spatial distribution, with most of the blocks clustered on one side of the asteroid near the multikilometer impact craters Mammoth and Lascaux (see Belton *et al.* 1995b for locations of named features). Yet these craters, which are obvious possible sources for the blocks (Lee *et al.* 1996), are thoroughly degraded and apparently quite old, possibly dating from the time of Ida's formation. As an alternative, we consider the possibility that the blocks originated far from their present positions and reimpacted at their current locations under the influence of Ida's exotic dynamical environment.

Several other observations hint that ejecta from impacts in the Ida system might be distributed far from the source craters. Small craters on Ida lack well-defined ejecta blankets: a full range of crater morphologies is seen on the surface of the asteroid, from fresh to severely degraded, but a corresponding range of ejecta blankets is not observed (Sullivan *et al.* 1996). Crater rims on Ida appear narrower than their lunar counterparts of similar size (*ibid.*), suggesting that target strength or other nongravitational factors play a significant role in the formation of craters up to 1 km in diameter. In the most extreme example, the interpretation of a crater chain and a possible ejecta block on Ida's tiny moon Dactyl (Veverka *et al.* 1994, Chapman *et al.* 1994), both presumably due to debris derived from Ida, suggest that ejecta from hypervelocity impacts can be distributed far and wide across the Ida/Dactyl system.

In this paper we consider the reaccretion and escape of ejecta on Ida and Dactyl, with the aim of predicting dynamical effects on surface morphology. Previous studies of the dynamical environments of Phobos and Deimos demonstrated appreciable variations over the surfaces of these satellites in the probabilities of ejecta escape and reimpact. Dobrovolskis and Burns (1980) employed a two-dimensional simulation of the restricted three-body problem to explore the effects of rotation, shape, and the gravitational perturbation due to Mars on the trajectories of particles launched from Phobos and Deimos and the possible influence of these factors on the surface morphology of the martian moons. Davis *et al.* (1981) extended this analysis to the three-dimensional case, modeling the satellites as uniform triaxial ellipsoids. Impact ejecta distributions were explicitly modeled by Davis *et al.* (1981) who showed that variations in effective surface gravity due to the tidal forces of Mars, and to a lesser extent the shape and rotation of the satellites, produce marked asymmetries in predicted morphologies of ejecta blankets. Banaszkiewicz and Ip (1991) performed a statistical study by launching particles from random locations on the satellite surfaces, demonstrating large variations in reimpact probability for each of the martian moons. Although each of these studies predicted that dynamical effects might be observable in the surface morphologies of Phobos and Deimos, no supporting evidence was found in Viking images of these small bodies (Thomas, 1979, Veverka and Thomas 1979). One possible explanation is the proximity of Mars; ejecta which ''escape'' the satellites remain bound to the primary, and may reimpact the satellites on time scales as short as 10^2 to 10^4 yr (Soter 1971). Ejecta reaccreted from Mars orbit might efficiently mask asymmetries predicted from dynamical studies of ejecta retention and escape on much shorter time scales.

The situation is quite different for main belt asteroids such as Ida. For one thing, ejecta which escapes in this case can be considered to be permanently lost to the system. Second, tidal forces due to close orbit about a massive planet can be neglected. Most important, Ida's very rapid rotation and highly elongated shape can be expected to produce marked effects on the dynamics of ejecta reaccretion and regolith redistribution. The rotation period of Ida is only 4.63 hr (Binzel *et al.* 1993), compared to the (synchronous) rotation periods of 7.65 and 30.31 hr for Phobos and Deimos (Burns 1986). In fact, Ida's rapid spin places it in the top 10% of measured asteroid rotation rates (Lagerkvist *et al.* 1989). Moreover, the elongation (a/b, for the best-fit triaxial ellipsoid) for Ida is 2.35, compared with values of 1.26 and 1.25 for Phobos and Deimos (Thomas *et al.* 1996, Burns 1986).

In the sections which follow we first examine the effects of rotation, launch location, and initial launch velocity for ejecta reaccretion on an ideal triaxial ellipsoid with Ida's approximate shape and density before using a more realistic model of the asteroid to study in some detail the ejecta distribution resulting from a specific crater on Ida: the Azzurra basin, which appears to be the most recent major impact event and in our view the best candidate for the source of the ejecta blocks. Finally, we consider the disposition of ejecta escaping from both Ida and Dactyl, estimate erosion rates and lifetimes against catastrophic disruption,

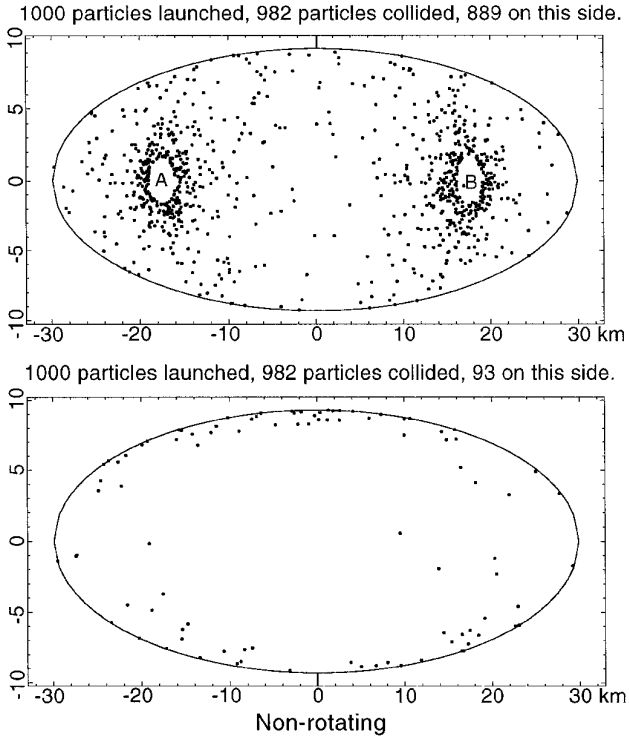

FIG. 1. Ejecta reaccretion simulation for a nonrotating ellipsoid with the dimensions and presumed density of Ida. The north pole (vertical line) is at the top of the figure in the upper diagram and at the bottom in the lower diagram, which shows the opposite side of the asteroid. Dots show the locations of reimpact for particles launched from the positions labeled A and B with a minimum speed of 4.7 m/sec. Compare with Fig. 2.

and speculate on the ultimate fate of these intriguing small objects.

2. EJECTA REACCRETION

The trajectories of projectiles launched from the surface of a small, rapidly rotating and irregularly shaped asteroid like Ida can be surprising and counterintuitive. For example, imagine an astronaut hurling rocks into space from the narrow end of Ida (180°E). With a gentle toss, a rock thrown in the direction of rotation lands (after an unearthly delay) in front of the astronaut, in the direction in which it was thrown. Thrown faster, a rock hurled in the same direction will appear from the surface to bend upward, and reimpact (after a considerably lengthier delay) behind the astronaut. All attempts to directly hit a distant surface in the rotation direction, like Regio Palisa, are futile, despite the fact that our astronaut could easily heave the rock with sufficient speed to escape Ida entirely. In contrast, it would be trivial to reach the opposite end of the asteroid by throwing a rock in the direction opposite to Ida's rotation, and an athletic astronaut might even be able to follow with a sufficiently large leap. (For perspective, an astronaut would need to exercise care in order to walk on the surface of Dactyl, as an overly energetic step would lead to permanent departure.)

In order to gain intuition about the dynamics of orbits near Ida, it is useful to examine separately the effects of shape, rotation, launch location, and initial launch speed. We will defer consideration of Ida's complex shape and begin by assuming a simple triaxial ellipsoid with semimajor axes of 29.9, 12.7, and 9.3 km (Thomas *et al.* 1996) and a density of 2700 kg m^{-3}.

2.1. Ejecta Blanket Morphology

Figures 1 and 2 show the effect of rotation on the distribution of ejecta launched at low velocities from two specific points on the leading and trailing surfaces of a rotating triaxial ellipsoid with the dimensions of Ida. A total of 1000 test particles were launched in each of these simulations, and their orbits were integrated in the (rotating) reference frame of the asteroid by computing the gravitational potential of the ellipsoid (Kellogg 1929) and updating the positions, accelerations, and velocities at each time step. The numerical integration is followed until the mass-

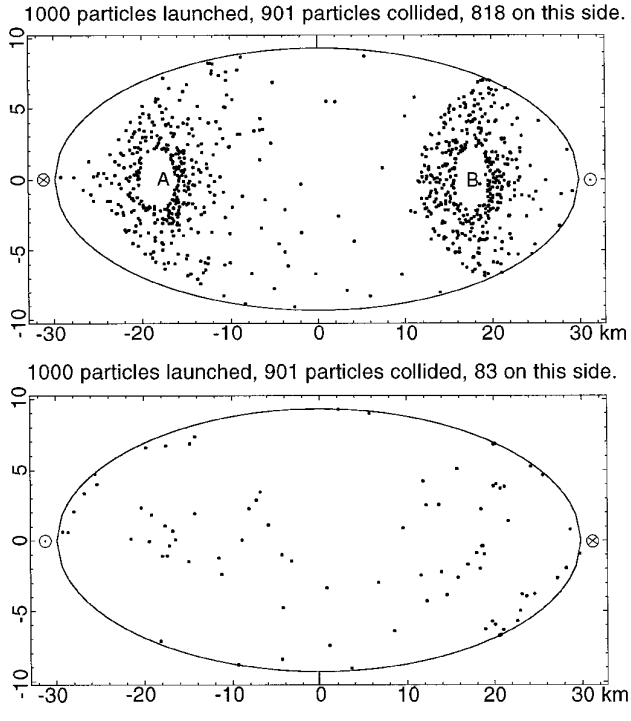

FIG. 2. Ejecta reaccretion simulation for an ellipsoid rotating at the spin rate of Ida. The rotation direction is indicated by symbols depicting motion toward the observer (dot within circle) and away from the observer (cross within circle). The north pole (vertical line) is at the top of the figure in the upper diagram and at the bottom in the lower diagram, which shows the opposite side of the asteroid. Dots show the locations of reimpact for particles launched from the positions labeled A and B with a minimum speed of 4.7 m/sec. Compare with Fig. 1.

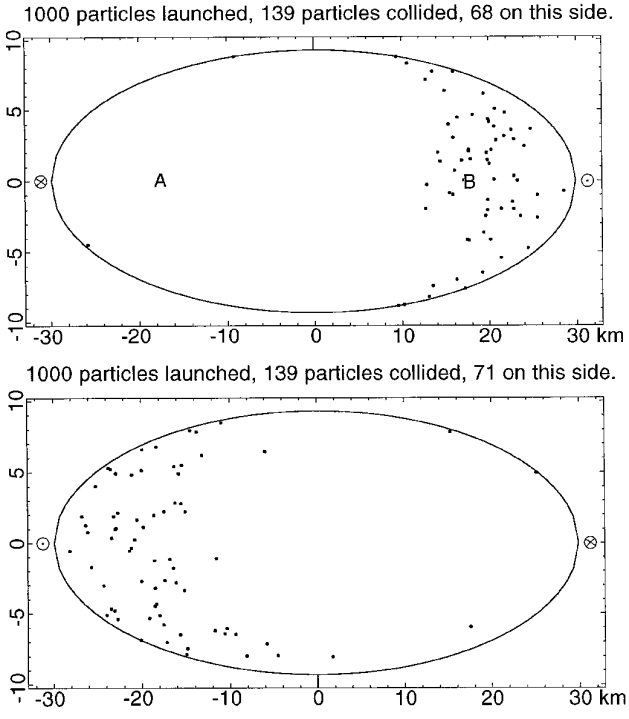

FIG. 3. Impact locations for particles launched from positions A and B at a minimum speed of 19 m/sec. Compare with Fig. 2.

less particles either collide with the central body, or escape. A particle escapes when it reaches a distance of more than 500 km with a binding energy (total energy = kinetic energy + potential energy) larger than the energy of a particle at rest at 10,000 km from the central body—the limit to the region where we consider our two-body approximation to be a good representation of reality.

The test particles are launched with a fixed inclination of 45° and with speeds drawn at random according to a power-law distribution between V_0 and V_{esc}, where V_{esc} = 18.7 m/sec is the ''average escape velocity'' calculated from the total mass of the ellipsoid and the geometric mean of the radii. The exponent of the (integral) velocity distribution for this simulation is $e_v = 1.2$, which is appropriate for unconsolidated surface materials such as dry sand (Housen *et al.* 1983, Andrews 1975). The diameter of the ''crater'' is determined by the minimum launch velocity, V_0, which is chosen for convenience in this case to be 0.25 V_{esc}, or 4.7 m/sec.

In the nonrotating case (Fig. 1), the locations where the particles reimpact the surface (shown by dots) are symmetric across the asteroid. Most of the particles are clustered close to the launch locations at these low velocities, and little ejecta escape. The situation is altered when the ellipsoid is rotated at the spin rate of Ida (Fig. 2). Ejecta are more widely dispersed on both the leading and trailing surfaces, reaching the opposite side of the asteroid. A significantly greater fraction of the ejecta escapes (10%, as opposed to only 2% in the nonrotating case). The ejecta blanket of the trailing crater (crater A) is notably asymmetric, with more ejecta on the right (trailing) side than on the left. The ejecta distributions resulting from both the trailing and leading (crater B) launch locations exhibit sharp cutoffs along the leading margins; particles launched at higher speeds in the direction of rotation are catapulted by the rotational velocity to escape or orbit. Similar results were obtained for ejecta distributions on Phobos by Davis *et al.* (1981, Fig. 5).

At higher initial launch velocities, fewer particles are retained and ejecta become more widely dispersed until, at speeds approaching V_{esc}, no recognizable ejecta blankets can be associated with any specific launch location. The fate of high speed ejecta (V_0 = 18.7 m/sec) from our two test craters is shown in Fig. 3. Most of the particles launched from the leading surface (crater B) escape. The fraction of ejecta which is retained is derived preferentially from the rotational trailing surface (crater A), but the landing sites are clustered on the rotational leading surfaces of both sides of the asteroid. This ''rotational sweeping'' is the result of recapture of ejecta which have gone into orbit for times that are long in comparison to the rotation period of Ida.

The effects of rotation are minimized at the poles. Figure

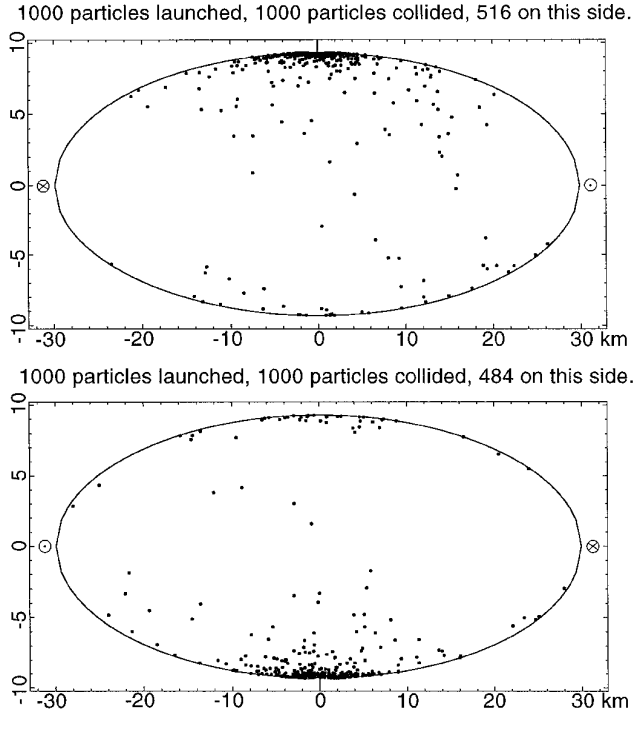

FIG. 4. Impact locations for particles launched from the north pole (indicated by a vertical line at the top of the figure in the upper diagram and at the bottom in the lower diagram, which shows the opposite side of the asteroid) with a minimum speed of 4.7 m/sec.

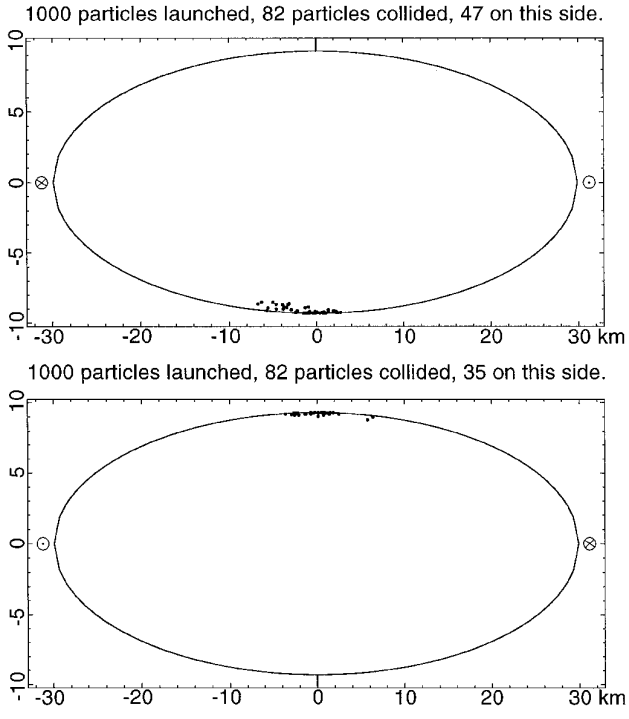

FIG. 5. Impact locations for particles launched from the north pole (indicated by vertical line) at a minimum speed of 19 m/sec. Compare with Fig. 4.

4 shows a simulation of an impact crater located at a rotational pole of Ida with the low initial launch speeds used in Figs. 1 and 2. The morphology of this ejecta blanket is virtually indistinguishable from the nonrotating case. At initial launch speeds comparable to the average escape velocity (V_0 = 18.7 m/sec), the ejecta "blanket" from a crater at the north pole is found on the opposite end of the asteroid, in the south polar region (Fig. 5).

Craters located at the ends of Ida (0°E and 180°E) have ejecta blankets which are most severely modified by rotational effects. Figure 6 shows a simulation of an impact crater near the 180°E end of Ida, i.e., at the location of our hypothetical stone-throwing astronaut. Because debris thrown in the direction of rotation loops back in the direction opposite to that in which it is thrown (relative to the surface), the ejecta blanket is confined to the rotational trailing surface, as shown by the figure. Ejecta launched from this location at initial speeds comparable to the average escape velocity never return.

2.2. *Regolith Redistribution*

To determine the cumulative effect of impacts occurring all over the asteroid, we have run a series of simulations in which particles are launched from random locations on the surface of the model asteroid with randomly chosen azimuthal directions and a constant inclination angle of 45°. The effects of ejection velocity are examined by choosing a constant initial launch speed for each numerical experiment. Ten-thousand particles are tracked in each simulation, and the locations and times of reimpact are recorded along with the launch locations of particles which are retained.

In the first example (Fig. 7), particles are given an initial velocity of 0.5 V_{esc}, or 9.4 m/sec. About 89% of the particles launched at this low velocity reimpact the asteroid (over 80% during the first rotation period; Fig. 8), and their distribution is random—as expected for these short hops across the surface of the model asteroid. The few (9%) particles that attain orbit for times longer than the rotation period show distinctly nonrandom spatial distributions in both their landing and launch sites, with clusters near the leading and trailing ends, respectively.

In contrast, only 5% of particles launched at 22.7 m/sec eventually return to the model asteroid. The locations of their collisions in this higher velocity case are sharply nonuniform, most occurring on the leading surfaces of both sides (Fig. 9). As can be seen from the plot of orbit times (Fig. 10), none of these particles reimpact immediately. The particles with the shortest flight times remain in orbit for durations equivalent to two asteroid rotation periods. Some particles stay in orbit for periods of up to a year before being reaccreted. The particles which do not escape in this case are launched preferentially in a retrograde direction from the rotational trailing surfaces, so that their effective initial launch velocities are at a minimum (Fig. 11).

The similarity between both Figs. 3 and 9 and the spatial distribution of ejecta blocks on Ida suggests that a dynamical mechanism could be responsible for the distribution of the blocks observed on Ida's surface. The blocks might have been preferentially swept up onto the rotational leading surface of Ida visible in the Galileo high resolution mosaic, provided that they were launched at speeds comparable to the asteroid's average escape velocity from an impact or impacts located on a rotational trailing surface. As it turns out, a large and evidently fresh crater is observed on the trailing surface of the far side of Ida; the best candidate for the source of the blocks is the crater Azzurra.

2.3. *Azzurra Simulation*

Azzurra is a ~10-km diameter basin located at 30°N, 220°E on the side of Ida opposite to that imaged at high resolution. It was presumably formed by a major impact event. No high resolution images of this region were obtained, but an indication that Azzurra might be relatively young is provided by a subtle color difference between the interior of the crater and the surrounding terrain (Fig. 12). Azzurra and the regions immediately east and north of the crater are somewhat less red and brighter at visible

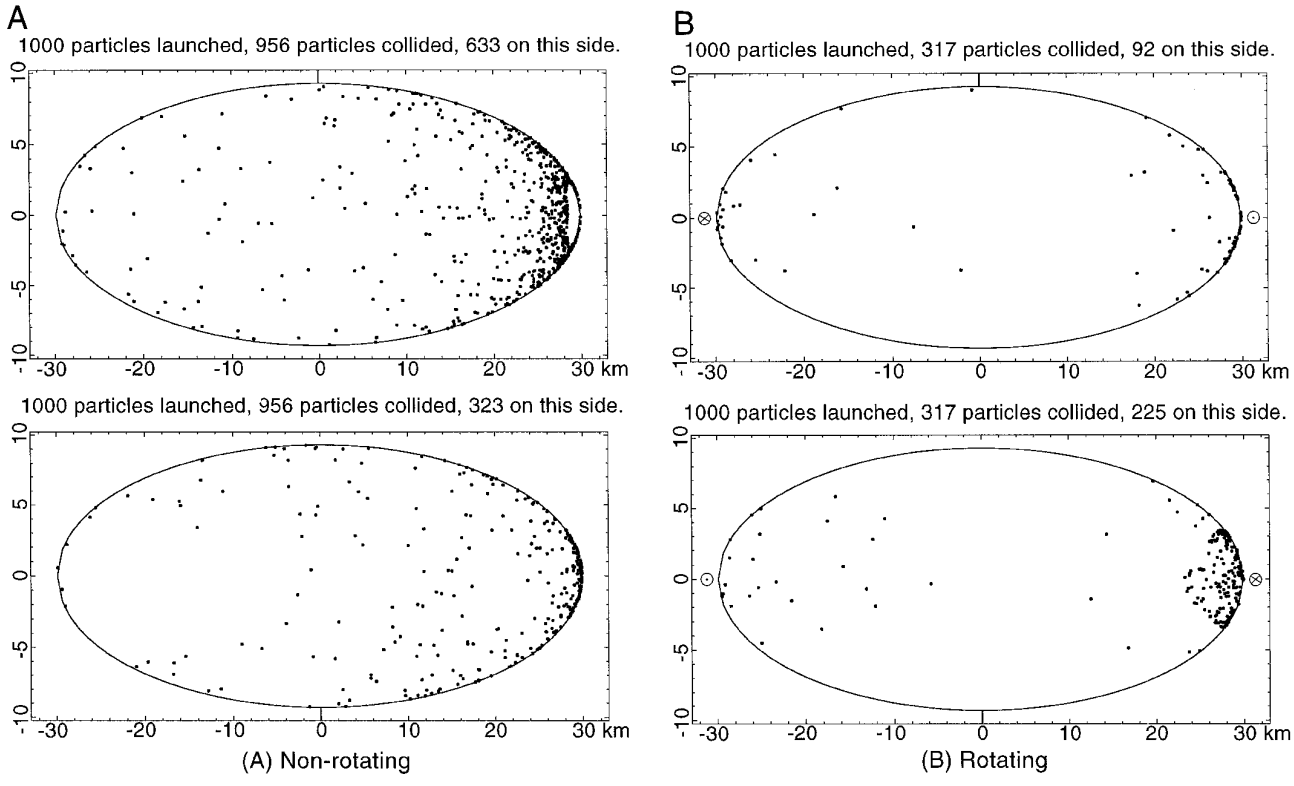

FIG. 6. Ejecta reaccretion simulation for the case of launch from the end of Ida, near the axis of elongation. (A) Nonrotating case. (B) Case of rotation at the spin rate of Ida.

wavelengths, and have a deeper 1-μm absorption than Ida's average surface. These characteristics are shared by a few of the freshest appearing and presumably youngest craters on Ida and are interpreted to indicate recent exposure of materials which are unaltered by the space environment (Sullivan *et al.* 1996). The color anomaly may extend across the polar region and be continuous with a similar spectral unit found at high northern latitudes on the opposite side of the asteroid. If this "blue" unit corresponds to ejecta from the Azzurra impact, then its proximity to the crater indicates launch speeds of a few meters per second, consistent with predictions of gravity-dominated crater scaling for multikilometer craters (Asphaug *et al.* 1996), and the asymmetry of the deposit implies that ejecta emplacement was substantially modified by the rotation and shape of Ida.

We calculate the trajectories of particles launched from Azzurra crater by assuming a more realistic model for the shape of Ida (Thomas *et al.* 1996), and filling the volume with a uniform grid of point masses such that the total equals the mass of the asteroid for our assumed density of 2700 kg/m^3. The acceleration of a test particle is computed in an inertial reference frame as the vector sum of the accelerations due to each of the point masses, and the positions and velocities of the test particle and the (rotating) shape model are updated at each time step (see Durda 1996, for details of the integration method).

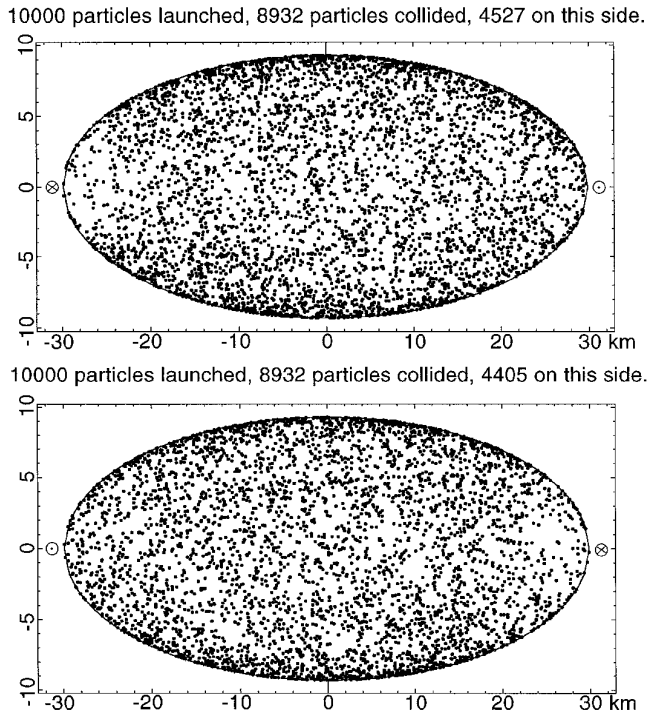

FIG. 7. Reimpact sites of particles launched at 9.4 m/sec, or half of the average escape velocity, from random locations on the surface of an ellipsoid with the rotation rate and dimensions of Ida.

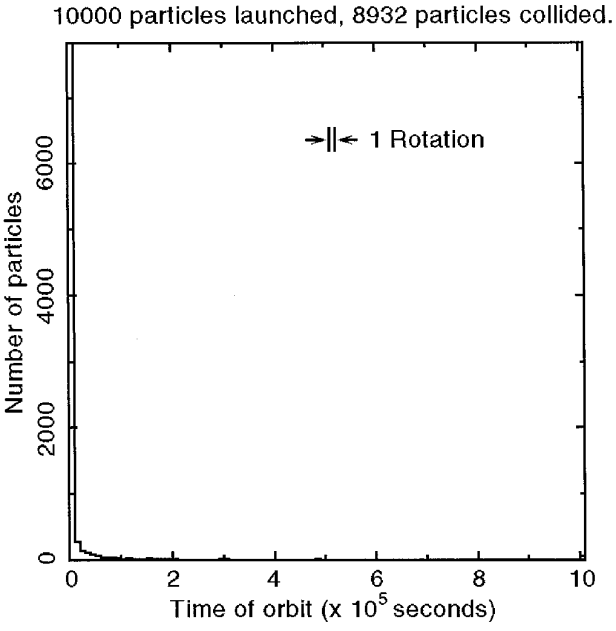

FIG. 8. Orbit times for particles returning to the surface in the low ejection velocity case shown in Fig. 7.

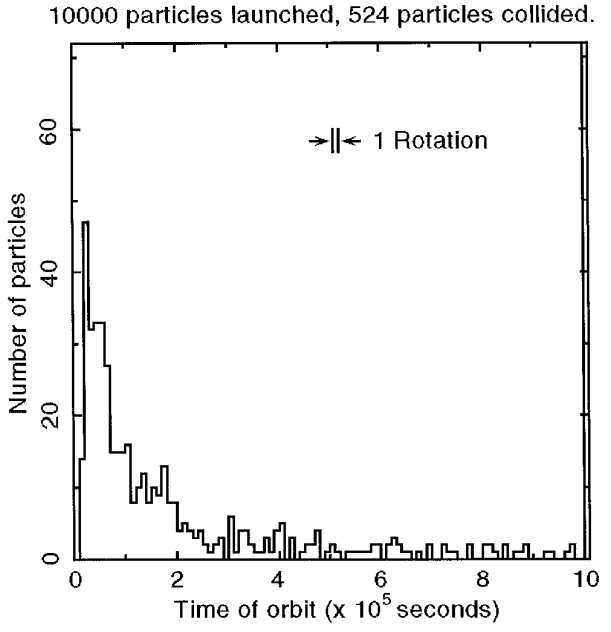

FIG. 10. Orbit times for particles returning to the surface in the high ejection velocity case shown in Fig. 9. All particles launched at 22.7 m/sec spend a minimum time in orbit which is greater than the asteroid's rotation period.

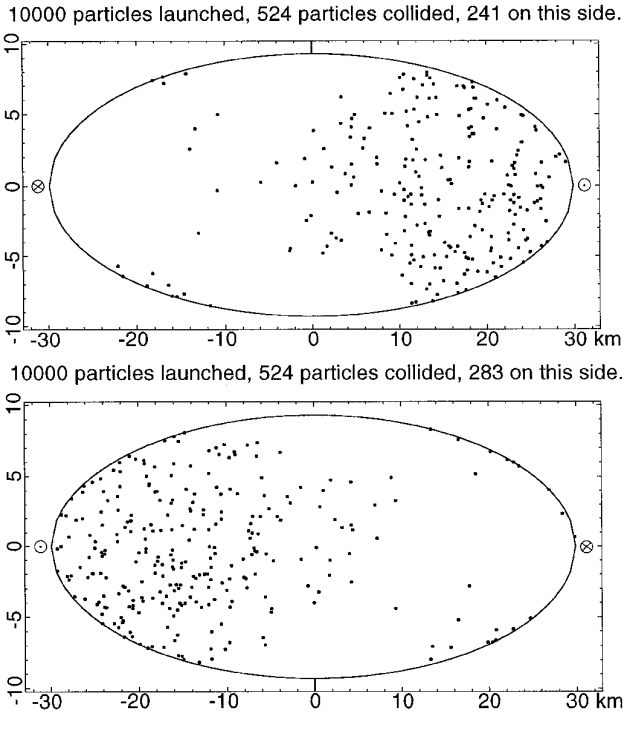

FIG. 9. Reimpact sites of particles launched from random locations at 22.7 m/sec. The landing locations in this high velocity case are sharply nonuniform, most occurring on the leading surfaces of both sides of the asteroid.

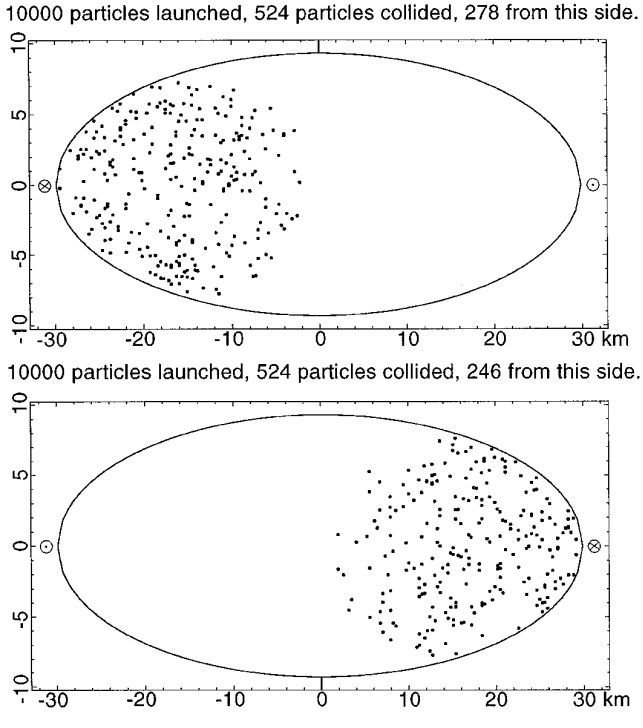

FIG. 11. Launch locations of particles retained on the ellipsoid after launch at 22.7 m/sec (i.e., for the case shown in Figs. 9 and 10).

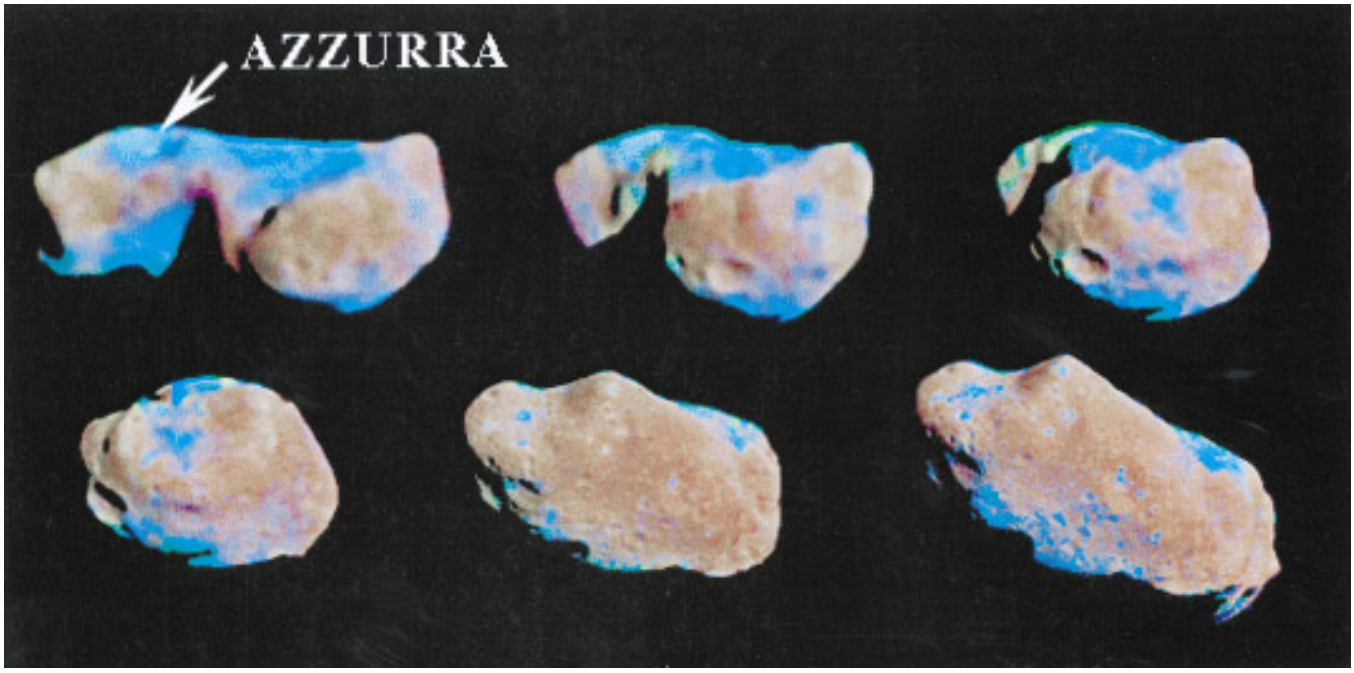

FIG. 12. Enhanced color ratio image of Ida, showing the distribution of the "blue" spectral unit (for detailed description see Veverka *et al.* 1996a).

Figure 13 shows the reimpact sites computed for 1000 particles ejected from Azzurra with initial launch speeds ranging from 5 to 15 m/sec with an exponent of $e_v = 1.2$. This figure shows a series of views of the asteroid from perspectives similar to that of Fig. 12 and should be directly compared with the color observations. The ejecta distribution predicted by the numerical simulation is qualitatively similar to the spatial distribution of the blue spectral unit in several important respects. The model predicts that the bulk of the ejecta should fall to the north and east of Azzurra, while little should land to the west of the crater, i.e., in the direction of rotation. Few particles are expected to impact on the ends of the asteroid, in agreement with the color unit boundaries in the western hemisphere. Azzurra ejecta is predicted to extend across the north polar region of Ida, so that it should be visible at high northern latitudes

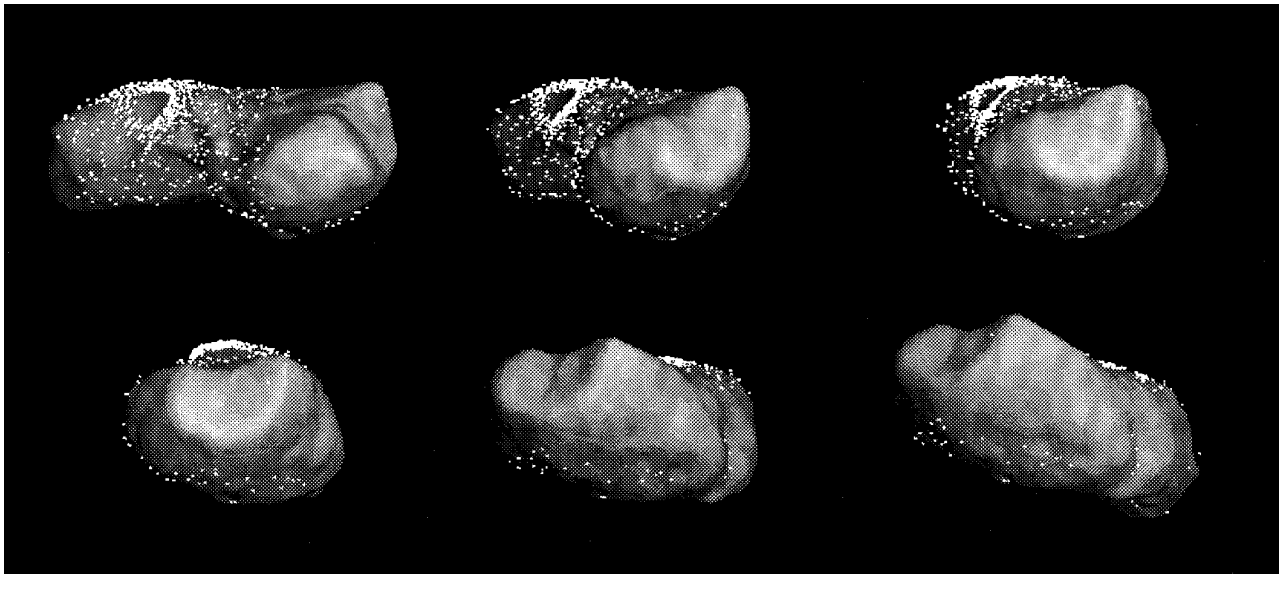

FIG. 13. Ejecta reaccretion simulation for particles launched from the Azzurra crater. Compare with Fig. 12.

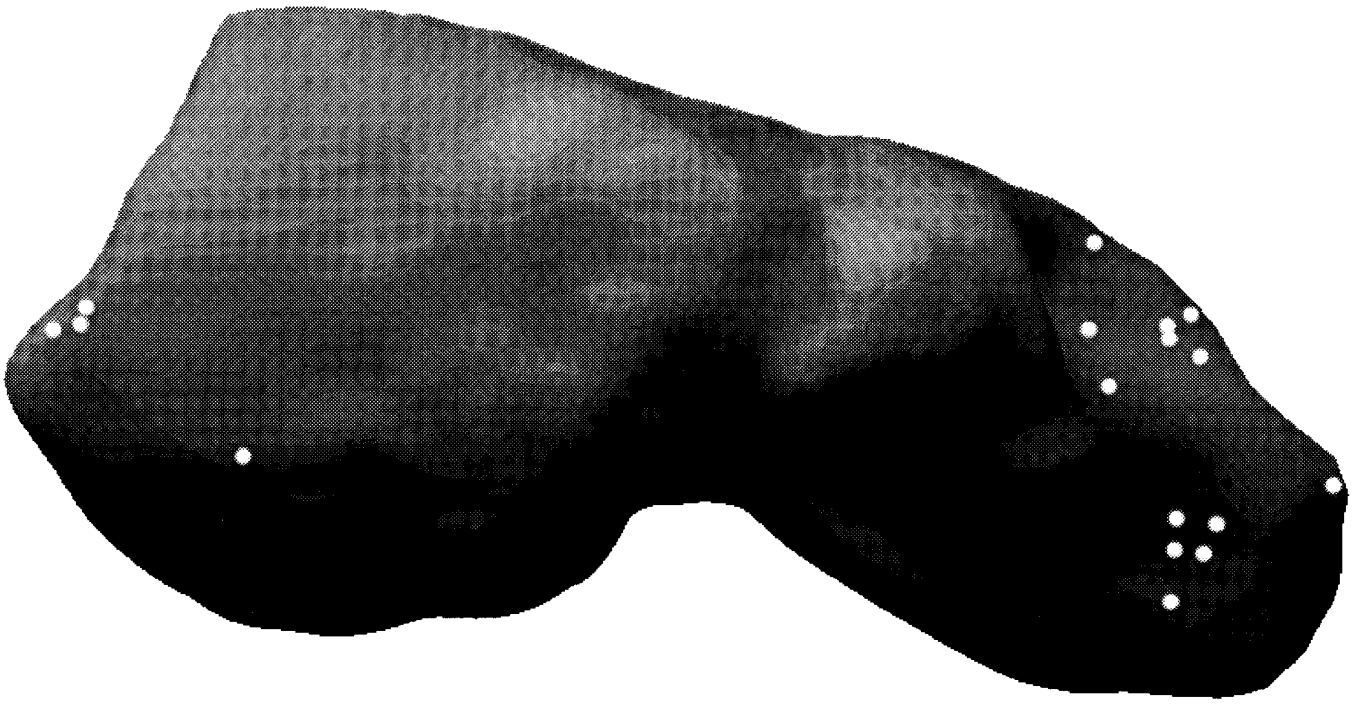

FIG. 14. Distribution of the 17 largest and most easily identified ejecta blocks on Ida. Compare to Fig. 15.

in eastern hemisphere views of the asteroid as seen in the color observations. A small number of particles impact in the southernmost reaches of Regio Palisa, again corresponding to the color anomaly shown in Fig. 12. The agreement between the modeling results and the distribution of the blue spectral unit strongly supports the conjecture that the color unit represents ejecta emplaced on ballistic trajectories from the Azzurra impact site.

One particular case of Azzurra ejecta reimpacts with a spatial distribution which closely matches the observed locations (Fig. 14) of large ejecta blocks on Ida. The fate of particles launched from the Azzurra crater at speeds just sufficient to reach the opposite side of the asteroid is shown in Fig. 15, a view of the eastern hemisphere of Ida from a perspective similar to that of the Galileo high-resolution image mosaic. Launch speeds in this simulation were randomly drawn with equal probability from a range restricted to 9 to 11 m/sec. Most of the ejecta launched at these speeds follow simple ballistic trajectories and reimpact near the crater, but the particles which are launched in the rotation direction are lofted far enough from Ida so that the asteroid rotates beneath them before they recollide. These particles follow retrograde trajectories to reach the side of Ida seen in the Galileo high resolution observations, and reimpact with a distinctive spatial distribution: particles are predicted to be preferentially swept up onto the leading rotational surface (longitudes 100° to 180°E) but are notably absent from the broad plain (Regio Palisa) on the adjacent trailing surface (longitudes 20° to 100°E). A second, smaller cluster is predicted to fall on the margin of Regio Palisa near the prime meridian—longitude 0°E. These are particles which received a ''gravity assist'' from Ida's rotational velocity as they passed over the Vienna Regio end of Ida and looped back in the rotation direction instead of continuing toward the Mammoth/Lascaux region (cf. Fig. 16). Comparison with the observed distribution of ejecta blocks (Fig. 14) shows excellent agreement, demonstrating that the boulders could have been launched at relatively high speeds (~10 m/sec) from the Azzurra impact basin.

3. ESCAPE OF EJECTA

As we have seen, ejecta retention on a rapidly rotating nonspherical body depends on both launch location and initial velocity. We can employ the realistic shape model of Thomas *et al.* (1996) to estimate the fraction of ejecta launched from random surface locations which is retained by Ida as a function of initial launch speed (Fig. 17). Here we define ''retained'' to include particles which remained in extended orbits about Ida before reaccreting; particles were considered to have escaped only when their distance from Ida exceeded 500 km and their total energy was positive. The complexities of this curve which are due to Ida's irregular shape can be seen by comparison with the ejecta retention rates predicted for the triaxial ellipsoid

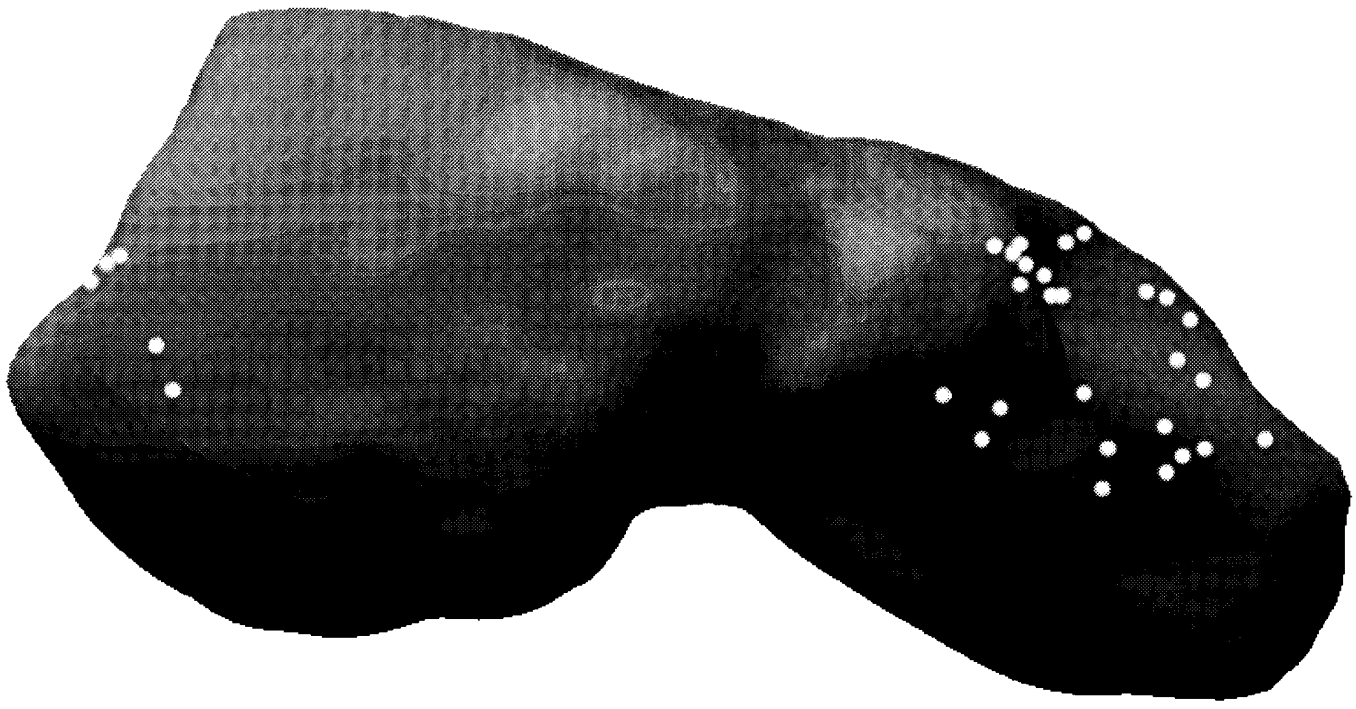

FIG. 15. Landing locations on the side of Ida seen at high resolution for particles launched in the direction of rotation from the Azzurra crater at speeds near 10 m/sec. Compare to Fig. 14.

model. In particular, particles launched from the deep depression near Ida's south pole fail to escape when launched at an inclination of 45° even with speeds of several tens of meters per second, due to the remarkable shape of the asteroid in this region. This depression forms an efficient trap of impact-derived regolith despite the fact that it corresponds to a local gravitational minimum (Thomas *et al.* 1996). Shown for reference in Fig. 17 is the escape velocity for a nonrotating sphere with Ida's assumed mass and density. Significant erosion takes place at launch speeds well below this average, while a small but interesting fraction is retained at higher speeds.

For the case of launch from Dactyl, there are four possible outcomes: particles may (1) reimpact the satellite, (2) collide with Ida, (3) escape the system, or (4) go into orbit around Ida for extended periods. The relative proportions of each of these possibilities depends on the semimajor axis, inclination, and eccentricity of Dactyl's orbit and the orbital phase of Dactyl (the position of the satellite in its orbit of Ida) as well as the launch direction and speed. We investigate the fate of ejecta from Dactyl by tracking the positions of test particles launched from random locations on a 1.5-km diameter sphere with a density of 2700 kg m^{-3} in orbit about a rotating triaxial ellipsoid as previously described. For each initial velocity, 100 particles are launched from each of 10 randomly drawn orbital phases and followed for 5,000,000 sec (300 asteroidal rotation periods). Particles which have not collided or escaped at the end of these two months are considered to have gone into orbit, although the number of orbiting particles counted in this way of course decreases with longer integration times. The experiments were performed three times with different random number seeds, and the results combined to obtain mean outcomes.

Results are presented for two different sets of satellite orbital elements, both of which are consistent with the Galileo constraints on Dactyl's orbit (Belton *et al.* 1995). Figure 18 shows the fate of ejecta launched from a prograde orbit (i.e., in Ida's rotation direction) with a semimajor axis of 106 km, 10° inclination, and eccentricity of 0.2. Ejecta is retained on Dactyl only if launched at speeds less than 1 m/sec. More than half of the particles launched at 1.4 m/sec go into orbit around Ida for periods longer than the integration time of two months. At slightly lower launch speeds, particles are scattered by gravitational interactions with Dactyl and escape the system (these particles remain in orbit when Dactyl is given a negligible mass). At launch speeds slightly higher than 1.4 m/sec, particles tend to escape after close encounters with Ida. Most of the particles launched at higher speeds (up to 20 m/sec) eventually impact Ida, which would be a significant sink of material eroded by impact cratering on Dactyl or resulting from the catastrophic disruption of a larger precursor satellite (Davis *et al.* 1996).

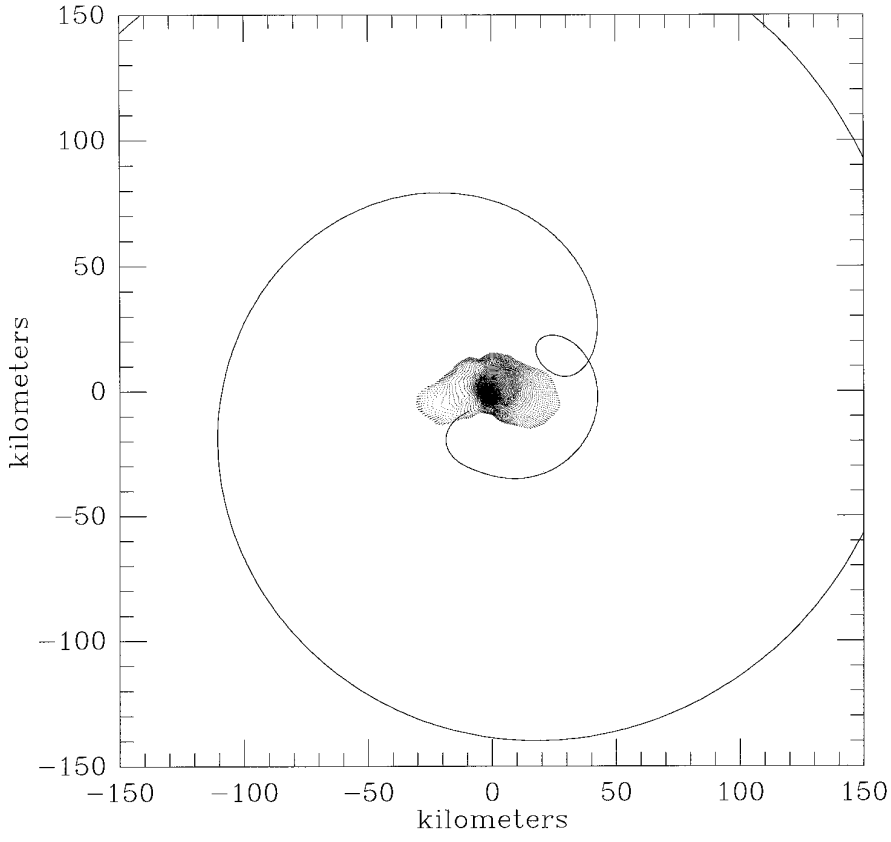

FIG. 16. Trajectory of a test particle launched from the Azzurra impact basin, plotted in the reference frame rotating with Ida. This particle was initially launched on a prograde orbit (i.e., in the direction of Ida's rotation) with a speed of 10.3 m/sec and inclination of 45°. From the point of view of an observer on Ida, the particle follows an apparently retrograde trajectory and receives a ''gravity assist'' from Ida's rotation, passing close by the surface before escaping the asteroid. Particles launched under slightly different initial conditions may reimpact Ida on the rotational trailing surface (the location of a secondary cluster of large ejecta blocks on Ida) or continue along retrograde trajectories to be swept up on Ida's rotational leading surface (the location of the most prominent cluster of ejecta blocks).

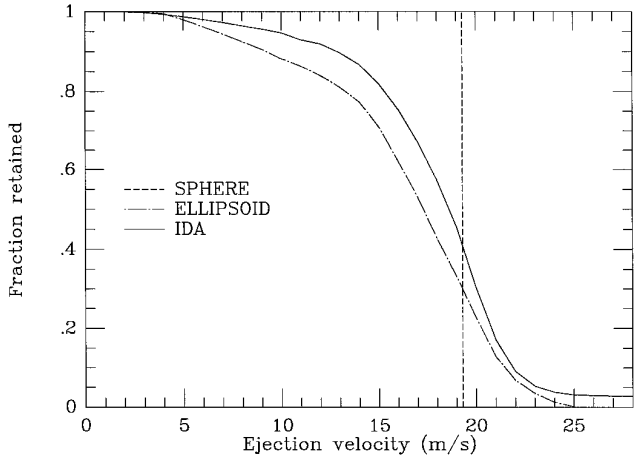

FIG. 17. Ejecta retention rates for particles launched from random locations on the surface of Ida with an inclination of 45°, as a function of initial launch speed. Also shown are regolith retention rates for the triaxial ellipsoid and a nonrotating sphere of Ida's volume and presumed density.

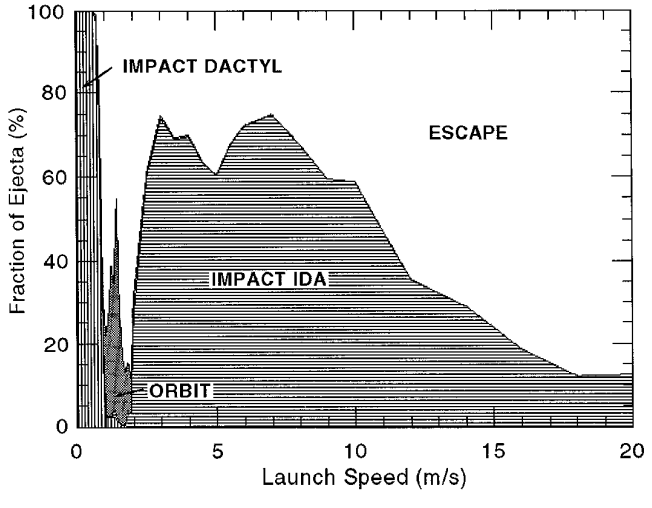

FIG. 18. Fate of ejecta launched from Dactyl, assuming nominal satellite orbital elements (a = 106 km, e = 0.2, i = 10°). The vertical height of each field represents the proportion of particles with the specified outcome. The statistical uncertainty in the number of particles escaping at 10 m/sec is ±9%.

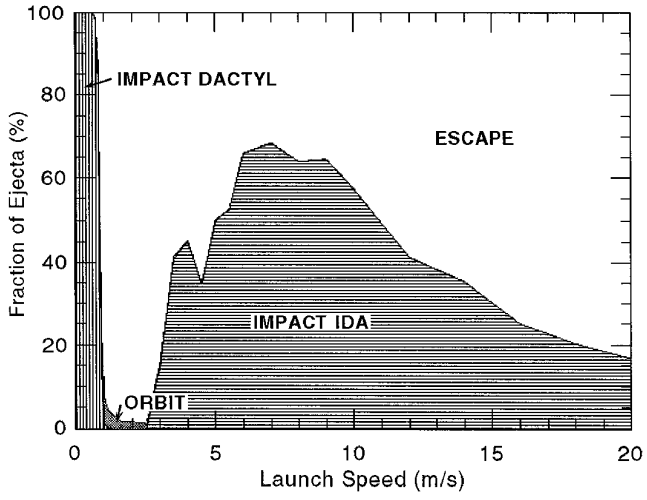

FIG. 19. Fate of ejecta launched from Dactyl, assuming an eccentric orbit for the satellite (orbital elements: a = 340 km, e = 0.8, i = 10°; density of Ida, 2100 kg m^{-3}).

Figure 19 assumes that Dactyl is on a prograde orbit which is highly eccentric (e = 0.8) and has a semimajor axis of 340 km. These orbital elements correspond to an Ida density of only 2100 kg m^{-3} (Belton *et al.* 1995), the value adopted for this simulation. Few particles launched from Dactyl enter into stable orbit around Ida in this case, since the launch locations are generally much farther from Ida. Again, about half of the particles ejected at initial speeds between 3 and 20 m/sec eventually impact Ida.

Surprisingly little of Dactyl's ejecta is eventually recaptured by the satellite, in contrast to the situations of Phobos and Deimos for which efficient reaccretion from long-lived "dust clouds" was predicted by Soter (1971). Most of the particles launched from a low eccentricity orbit at 1.4 m/sec, which enter relatively long term orbit around Ida (Fig. 18), ultimately escape when the integration time is extended to 5×10^7 sec (19 months). Possible reasons for the inefficiency of reaccretion include the highly nonspherical shape of the Ida in comparison to Mars, and the much larger relative mass (i.e., the ratio of the mass of the satellite to the mass of the primary) of Dactyl than either Phobos or Deimos. Dactyl's axial diameters are $\sim 1.6 \times 1.4 \times 1.2$ km (Veverka *et al.* 1996b), so assuming that Dactyl and Ida have equal densities yields a relative mass of $\sim 10^{-4}$ for Dactyl, compared to 2×10^{-8} for Phobos and 2.8×10^{-9} for Deimos (Burns 1986). Gravitational scattering by Dactyl efficiently clears the space surrounding Ida and makes it highly unlikely that another nearby satellite orbits the asteroid.

From Figs. 18 and 19 we can assume that the collision probability for material transported from Dactyl to Ida is on the order of 0.5 over the range of launch speeds of interest. An estimate of the collision probability for material transported in the reverse direction (from Ida to Dactyl) can be obtained from geometric considerations, by comparing the collision cross section of Dactyl to the area of a sphere with the radius of Dactyl's orbital semimajor axis. This approach yields a collision probability of about 1.4×10^{-5}. In our numerical simulations we have managed to hit Dactyl with projectiles launched from Ida a total of four times out of 200,000 trials, agreeing to order of magnitude with the estimate from geometric arguments. Note that these collision probabilities are calculated only for individual test particles. Capture of Ida ejecta by Dactyl could be enhanced if mutual collisions between ejecta particles or other mechanisms alter ejecta trajectories into stable Ida orbit (see discussion by Davis *et al.* 1996). Ejecta blocks and other debris from Ida may have impacted Dactyl and be visible in Galileo images of the tiny satellite (Veverka *et al.* 1994; Chapman *et al.* 1994), despite the low collision probability. In order to derive mass transfer rates between Ida and Dactyl we must first estimate the rates of erosion of the two asteroids.

4. EROSION RATES

4.1. Method

The rate of mass loss from a small asteroid through escape of impact ejecta is

$$\frac{dm}{dt} = \frac{d}{dt} \int \frac{d^2n}{dU\,dD} \rho V(U, D) F_{\rm esc}(U, D)\, dU\, dD, \quad (1)$$

where $n(U, D)$ is the total number of impacts occurring on the asteroid from impactors of diameter D and collision speed U, ρ is the target density, $V(U, D)$ is the volume of a crater excavated by an impactor of diameter D and speed U, and $F_{\rm esc}$ is the fraction of ejecta that escapes.

We obtain an analytic solution of (1) by assuming a constant impactor speed U and approximating $d/dt\ dn/dD$ as the product of the target collision cross section R^2, the size-frequency distribution of the impactor population $dN(D)/dD$, and an intrinsic collision probability P_i (assumed independent of the size of the impactors) to get

$$\frac{dm}{dt} = R^2 \times P_i \times \rho \int \frac{dN(D)}{dD} V(D) F_{\rm esc}(D)\, dD. \quad (2)$$

An appropriate choice for the impactor speed U is the root mean square collision velocity of impacts between the known asteroids and Ida, U_{RMS} = 3.92 km/sec (Bottke *et al.* 1994). As discussed in the Appendix, erosion rates for cratering in both the strength and gravity regimes are proportional to U raised to a power of up to 1.66, making the root mean square more appropriate than the mean collision velocity. Much more significant uncertainties in erosion

rate estimates are due to the fundamental lack of knowledge of the size-frequency distribution of impactors and the physical properties of Ida and Dactyl which govern the nature of impact cratering on these small objects. Various assumptions about the impactor population and the volume and velocities of ejecta produced by impacts into targets of different types yield erosion rate estimates which differ by orders of magnitude. Nevertheless, some quantitative limits can be placed on erosion rates by considering various extreme cases for assumed impactor populations and crater scaling laws.

The largest source of uncertainty is the unknown population of asteroids impacting Ida and Dactyl, both in terms of the flux of impactors and the relative numbers of large versus small particles (see discussion by Farinella and Davis 1994). The flux of impactors obviously affects the rate of erosion, but the morphological expression of erosion—whether the surface is sandblasted by small particles or has fewer big bites taken during large cratering events—is controlled by the slope of the impactor size-frequency distribution. We examine both of these possibilities by considering distributions dominated alternately by large and small particles. Each of the three models we employ for the population of asteroids impacting Ida is a double power-law distribution of the form (Belton *et al.* 1992)

$$\begin{aligned} dN(D) &= c_1 D^{q_1}\, dD, D < 175 \text{ m, and} \\ dN(D) &= c_2 D^{q_2}\, dD, D > 175 \text{ m.} \end{aligned} \tag{3}$$

For large diameters, $q_2 = -2.95$ is chosen to match that of the Palomar–Leiden Survey (Van Houten *et al.* 1970) and c_2 normalized so that $N(D > 50 \text{ km}) = 951$. For smaller particles, differential slopes of both -3.5 (Dohnanyi, 1969) and -4.0 are used, the latter providing a better match to the cratering record on Gaspra (Belton *et al.* 1992; Greenberg *et al.* 1994; Carr *et al.* 1994). For the $q_1 = -4$ distribution, the mass of impactors becomes infinite as impactor diameters approach zero, so we must choose a minimum projectile size below which the steep size-frequency distribution is assumed to no longer apply. One possible choice (Population 1) is a minimum diameter $D_{\min}$ of 1 m, forming craters in the diameter range 10 to 100 m near the resolution limit of the observations (~40 m/pixel). On the other hand, extending the steep size distribution down to $D_{\min} = 1$ mm (Population 2) means that as much mass is in the smallest particles as in the largest impactor considered to have caused erosion (and not catastrophic disruption) on Ida. This is the case of ''sandblasting'' the surface of the asteroid at a rate sufficient to soften the appearance of surface morphology on Ida and polish Dactyl into near-sphericity. At the opposite extreme, a population dominated by the largest particles (Population 3) is assumed when an exponent of $q_1 = -3.5$ is adopted, corresponding to a collisionally evolved population of asteroids with size-independent strength (Dohnanyi 1969). The minimum impactor size is immaterial in this case, so we can use $D_{\min} = 0$.

TABLE I
Disruption Time Scales for Various Impactor Populations, in Years

Impactor population	Ida	Dactyl	100-m block
1	2.0E + 09	2.5E + 08	3.3E + 07
2	2.0E + 09	2.5E + 08	3.3E + 07
3	2.0E + 09	4.1E + 08	1.8E + 08

We emphasize that these calculations pertain only to erosion, and not catastrophic disruption. An upper limit is imposed on the size of the largest impactor considered to have caused ''erosion'' by the requirement that the target not be destroyed by the projectile. The largest impactor sizes considered for Ida and for Dactyl are of course vastly different. The diameter $D_{\max}$ of the smallest projectile capable of destroying Ida or Dactyl is estimated by equating its kinetic energy $\frac{1}{2} MU^2$ with the specific energy S needed to destroy the target (assuming that half of the energy is partitioned into the target) to get

$$D_{\max} = (4S/\rho U^2)^{1/3} D_{\text{target}}, \tag{4}$$

where S is given in cgs units by (Housen *et al.* 1991; Marzari *et al.* 1995)

$$S = (2.1 \times 10^5 R^{-0.24} + 5.75 \times 10^{-6} R^{1.65}) \rho U^{0.35}, \tag{5}$$

assuming a size-dependent target strength and that target and impactor densities are equal. From (4) and (5) we find that the minimum diameters of objects colliding at 3.92 km/sec which could disrupt Ida, Dactyl, and a 100-m diameter block are 1960, 46, and 4 m, respectively. These impactor diameters will be used for the upper limits to the integral, Eq. (2). The relative importance of erosion versus catastrophic disruption for any given size-frequency distribution of impactors can be determined by comparing the time scale for erosion ($m/(dm/dt)$) to the time scale for disruption $[R^2 P_i N(D > D_{\max})]^{-1}$. Using the disrupter sizes and impactor populations derived above, we compute lifetimes against catastrophic disruption for Ida, Dactyl, and a 100-m ejecta block which are listed in Table I. Because they are partially shielded by the asteroid, Dactyl and blocks on Ida should survive for periods up to twice as long as indicated by this calculation, which applies to isolated objects. As discussed by Davis *et al.* (1996), Dactyl's disrup-

tion lifetime may be significantly shorter if the satellite is strengthless, compounding the conundrum of its continued survival.

The other major source of uncertainty is the amount of mass eroded by an impactor of any given size. Erosion caused by millimeter-sized particles can be assumed to be in the strength regime even in the case of large asteroids with low strength, but for shallower size distributions in which erosion is dominated by the largest impactors, numerical hydrocode results suggest that gravity scaling can apply to targets made up of solid rock if the strength is scale- or strain-rate dependent (Asphaug *et al.* 1996). Because the nature of cratering on small asteroids is unknown, our approach is to present results for both strength and gravity scaling in order to cover the range of possibilities. The crater scaling laws used here are taken from Holsapple (1993) and reflect three extreme assumptions for the nature of cratering and the properties of the target. First, we consider simple strength scaling appropriate to laboratory-scale cratering in soft rock, terming this model "rock." Scale- or strain-rate dependence of target strength may drastically increase the cratering efficiency, so neglecting these effects should yield lower limits to erosion rates. As shown in the Appendix, erosion by cratering in the gravity regime is proportional to g^{-e_v}, so that the mass eroded by similar-sized impactors can be vastly greater on Dactyl than on Ida, depending on the assumed value of e_v. For our calculations we will use gravity-scaling exponents of both $e_v = 1.66$ ("rubble," appropriate to gravity regime cratering in nonporous materials such as rock, wet sand, and water) and $e_v = 1.23$ ("sand").

4.2. Results for Ida and Dactyl

Erosion rate estimates for each of the assumed impactor populations and target types/cratering regimes are compiled in Tables II and III for Ida and Dactyl, respectively. In the case of Ida, mass erosion rates fall in the range of 10^6 to 10^7 kg yr^{-1} and are relatively insensitive to the choice of assumptions. These correspond to surface erosion rates of only 10^{-6} to 10^{-7} m yr^{-1}, i.e., between 1 and 10 Myr are needed to remove an average of 1 m in depth. The erosion lifetime of Ida at these rates is comparable to the age of the Solar System. Combined with the collision probability for individual particles derived in Section 3, these figures suggest a minimum mass transfer rate from Ida to Dactyl on the order of 20 to 200 kg yr^{-1}.

Mass erosion rates for Dactyl, in contrast, are strongly dependent on the cratering regime in which erosion is supposed to occur. Erosion of a "rock" Dactyl is insignificant except for the case of sandblasting by an impactor population dominated by small particles. In this case, the erosion lifetime is comparable to both the age of the asteroid and the time scale for catastrophic disruption, and erosion could produce profound effects on surface morphology. On the other hand, mass erosion rates predicted for cratering in the gravity regime are embarrassingly high, reaching 10^4 to 10^6 kg yr^{-1}. Predicted lifetimes of a "rubble" or "sand" Dactyl against erosion range from a few millions to a few hundreds of million years. While some of the material escaping Dactyl would be subsequently swept up by the satellite, most of this ejecta would be lost to space or devoured by Ida. Assuming that half of the ejecta escaping Dactyl eventually falls on Ida, whereas only $\sim 2 \times 10^{-5}$ of the particles launched from Ida impact the satellite (Section 3), the mass transferred from Dactyl to Ida exceeds the mass flux from Ida to Dactyl regardless of Dactyl's target type or cratering regime. Dactyl would have to collect at least 1% of the debris escaping Ida to

TABLE II
Erosion Rates for Ida

Impactor population	Erosion rate (kg yr^{-1})	Erosion lifetime (yr)
	Rock (strength regime)	
1	3.1E + 06	1.4E + 10
2	4.4E + 06	1.0E + 10
3	2.5E + 06	1.8E + 10
	Rubble (gravity regime)	
1	7.9E + 06	5.6E + 09
2	1.1E + 07	3.9E + 09
3	6.3E + 06	6.9E + 09
	Sand (gravity regime)	
1	1.8E + 06	2.4E + 10
2	2.6E + 06	1.7E + 10
3	1.5E + 06	3.0E + 10

TABLE III
Erosion Rates for Dactyl

Impactor population	Erosion rate (kg yr^{-1})	Erosion lifetime (yr)
	Rock (strength regime)	
1	1434	2.7E + 09
2	4022	9.6E + 08
3	383	1.0E + 10
	Rubble (gravity regime)	
1	640595	6.1E + 06
2	1.8E + 06	2.2E + 06
3	170352	2.3E + 07
	Sand (gravity regime)	
1	39001	9.9E + 07
2	109368	3.5E + 07
3	10371	3.7E + 08

balance the erosion rates predicted for impact cratering in the gravity regime. Because of its low gravity, Dactyl should be susceptible to both erosion and disruption on very short time scales unless it has substantial strength, and even a solid satellite should have difficulty retaining a regolith. A rubble- or sand-pile asteroid of Dactyl's small size would necessarily be much younger than the presumed age of Ida ($\sim 10^9$ years) and thus could not be a product of the disruption of the Koronis parent body as described by Durda (1996). If Dactyl is as old as Ida then it must be a solid rock, with the important implication that its remarkably rounded shape and smooth surface are not due to self-gravity or a thick regolith, but are the results of collisional modification over the lifetime of the satellite.

5. DISCUSSION

No evidence of a leading/trailing asymmetry in color or albedo was detected by the Galileo imaging observations of Ida. Because small particles are generally ejected at higher launch velocities than large particles, we would expect to find concentrations of fine regolith on the rotational leading surfaces of the asteroid by the same mechanism invoked to explain the distribution of boulders. Perhaps dust on Ida blends with the coarser regolith and is indistinguishable in color and albedo. Alternatively, the fine fraction of ejecta might be launched at speeds in excess of 25 m/sec and escape. Sandblasting of the surface by impactors with a steep size-frequency distribution could also provide a mechanism for regolith removal, with small impactors "cleaning" the soil generated in larger impact events.

Launch speeds on the order of 10 m/sec are required for the large ejecta blocks to have reached their current locations from the Azzurra impact site. Although large particles are generally the slowest component of the excavation flow of impact ejecta, the largest ejecta fragments are often products of spallation (Melosh 1989), which can be launched at much higher velocities and often compose the least shocked component of ejecta—that most likely to include intact blocks. While large ejecta blocks are expected to be present on Ida and similar-sized asteroids, such features are unlikely to originate on an object the size of Dactyl. Lunar and terrestrial cratering data indicate that 30–100-m-diameter blocks require source craters with diameters between 1 and 10 km (e.g., Moore *et al.* 1972, Lee *et al.* 1986). Such craters can be created on Ida by impactors in the diameter range 50–350-m for crater formation in the gravity regime. Assuming our most conservative impactor population (Population 3), the average production rate for 1-km-diameter craters on Ida is on the order of one per million years, while 10-km craters typically form on a 70-million-year time scale. Block production thus keeps pace with block destruction despite the relative paucity of large impactors, because of the much larger collision cross section of Ida in comparison to the size of the blocks. Large ejecta blocks should be rare or absent on much smaller asteroids, however, implying that any such blocks found on Dactyl were likely recently ejected from Ida. Launch velocities of the magnitude inferred for the ejecta blocks visible in the high resolution images of Ida are marginally sufficient to reach Dactyl, and mass transfer calculations suggest that the volume equivalent of a 25-m-diameter block is delivered to Dactyl from Ida every few million years. If the isolated positive relief feature on Dactyl is indeed a fragment of ejecta from Ida, it might not be the first "allochthonous terrain" discovered on a small asteroidal object: blocks on Deimos are anomalously large in comparison to the size of Deimos' impact craters (Lee *et al.* 1996) and could conceivably be ejecta from Stickney, a multikilometer crater on Phobos.

Debris from Ida which collides with its satellite will impact at speeds comparable to Dactyl's orbital velocity—a few meters per second. Such particles would be incapable of forming craters on competent rock, so the series of aligned craters visible on Dactyl could not be secondary impacts from Ida unless the surface of the satellite was quite soft. As we have seen, any regolith on Dactyl would be rapidly removed unless resupplied by Ida with an efficiency several orders of magnitude larger than estimates based on the trajectories of individual particles. Perhaps stochastic large impacts on Ida supply Dactyl with an ephemeral regolith: for example, if 1% of the volume of the Azzurra crater were deposited on Dactyl, a layer of regolith 10 m thick would result on the satellite. Alternatively, Dactyl's craters might have been created in hypervelocity impacts by main-belt and Koronis family asteroids, with the crater chain simply a chance alignment. If Dactyl is a solid body, then its shape has evolved from a presumably irregular fragment to an almost spherical figure by collision with a population of impactors too small to be detected by usual methods of crater counting. As the smallest object yet imaged by a spacecraft, the morphology of Dactyl is an important clue to the asteroid population at the smallest sizes.

6. SUMMARY AND CONCLUSIONS

In the preceding sections we have explored some theoretical aspects of escape and reaccretion of impact ejecta in the Ida/Dactyl system along with the implications of the results for the surface morphology of these smallest members of the Solar System. The findings summarized below may be generally applicable to other small asteroidal objects which rotate rapidly and are nonspherical in shape. One example (Geissler *et al.* 1995a,b) is Asteroid 433 Eros, the target of an impending orbital mission which will provide an opportunity to gather observations much more

thorough and detailed than the brief flybys of spacecraft Galileo.

1. The morphology of crater ejecta blankets and the distribution of impact-derived regolith on asteroids such as 243 Ida are significantly influenced by orbital dynamical effects due to their low gravity, nonspherical shape, and rapid rotation. At low launch speeds ($V \ll V_{esc}$), craters form well-defined ejecta blankets which are asymmetric in morphology between leading and trailing rotational surfaces and have sharp margins in the direction of rotation. The asymmetry is most pronounced for equatorial craters located near the axis of maximum elongation, and is minimized for craters located near the rotation poles. The net effect of cratering at low ejecta launch velocities is to produce a thick regolith which is evenly distributed across the surface of the asteroid.

No clearly defined ejecta blankets are formed when ejecta are launched at higher initial velocities ($V \sim V_{esc}$). Most of the ejecta escape, while the fraction which is retained is preferentially derived from the rotational trailing surfaces. These particles spend a significant time in temporary orbit around the asteroid, in comparison to the asteroid's rotation period, and tend to be swept up onto rotational leading surfaces upon reimpact. The net effect of impact cratering with high ejecta launch velocities is to produce a thinner and less uniform soil cover, with concentrations on the asteroid's rotational leading surfaces.

2. An extensive color/albedo unit which dominates the northern and western hemispheres of Ida is matched in detail by a numerical simulation of reaccretion of impact ejecta from a large and evidently recent crater (''Azzurra'') located on a rotational trailing surface on the side of Ida opposite to that imaged in high resolution observations. Initial ejection speeds required to match the color observations are on the order of a few meters per second, consistent with models (e.g., Asphaug *et al.* 1996, Nolan *et al.* 1996) that multikilometer craters on small asteroids form in the gravity-dominated regime and are net producers of locally retained regolith.

3. The distribution of large ejecta blocks observed in high resolution images of Ida fits a dynamical model in which Azzurra ejecta launched in the rotation direction at speeds near 10 m/sec are lofted over the asteroid on retrograde trajectories and swept up onto the rotational leading surface on the opposite side. Particles which pass close by Vienna Regio receive a gravity assist from the rotational velocity of the asteroid and loop back to form a secondary cluster on the margin of the rotational trailing surface. The high launch speeds required for these particles suggest that the ejecta blocks are probably products of spallation, rather than part of the lower speed excavation flow from Azzurra.

4. Ida's shape and rotation allow escape of ejecta launched at speeds far below the escape velocity of a nonrotating sphere of Ida's volume and presumed density. A small fraction of ejecta is retained when launched at speeds above the average escape velocity of Ida, particularly in the ''cave'' at high southern latitudes which forms an efficient trap of impact-derived regolith despite the fact that it corresponds to a local gravitational minimum (Thomas *et al.* 1996).

5. Most of the ejecta launched from Dactyl at speeds of up to 20 m/sec eventually fall on Ida. Particles ejected at speeds just barely exceeding Dactyl's escape velocity can enter relatively long term orbit around Ida, but few ultimately reimpact on the satellite. Low speed ejecta are efficiently placed into long term orbit when Dactyl's orbital eccentricity is small (0.2), but tend to rapidly escape when a more eccentric satellite orbit ($e = 0.8$) is assumed. Dactyl clears the space surrounding Ida both by capture of orbiting debris and by gravitationally scattering particles to escape Ida orbit.

6. Crater formation and erosion due to gravity-dominated cratering should be far more efficient on Dactyl than Ida, due to the low gravity of the tiny satellite. Current models for crater formation and the population of impacting asteroids suggest that erosion of Dactyl would take place on exceedingly short time scales if unconsolidated materials compose the satellite and gravity-scaling applies. If Dactyl is not a rubble or sand pile, and instead is a coherent object with substantial strength, then its shape has evolved from a presumably irregular fragment to its present remarkably rounded figure by collision with a population of impactors too small to be detected by counting visible craters on the satellite. As the smallest solar system object yet imaged by a spacecraft, the morphology of Dactyl is an important clue to the asteroid population at the smallest sizes.

APPENDIX: EROSION RATE CALCULATION

We obtain erosion rates for Ida and Dactyl by assuming a constant impactor velocity $U = 3.92$ km/sec and evaluating the integral

$$\frac{dm}{dt} = R^2 \times P_i \times \rho \int_{D_{min}}^{D_{max}} \frac{dN(D)}{dD} V(D) F_{esc}(D)\, dD, \qquad \text{(A1)}$$

where

R^2 = asteroid radius squared = target collision cross section
P_i = intrinsic collision probability for Ida (3.83×10^{-18} km^{-2} yr^{-1}, from Bottke *et al.* 1994)
ρ = asteroid density, assumed impactor density (2700 kg m^{-3})
$N(D)$ = number of impactors of diameter D
$V(D)$ = volume of crater excavated by impactor of diameter D
$F_{esc}(D)$ = fraction of ejecta escaping from impact of asteroid of size D.

Crater Scaling

We consider two extremes cases for the character of impact erosion, depending on whether the asteroids are assumed to be ''hard'' or ''soft'':

Strength Scaling. In the limit of high target strengths, small target sizes, or small impactor sizes, ejecta velocities should exceed the escape velocity of small asteroids such as Dactyl and Ida ($F_{esc} = 1$) and crater volumes are expected to increase linearly with impactor mass. In this case,

$$V(D)F_{esc}(D) = hD^3 \tag{A2}$$

for some constant h which depends on target strength and impactor velocity. A value of $h = 120$ is suggested by Holsapple (1993) for soft rock impacted at 3.92 km/sec (the crater volume increases as $U^{1.65}$). The mass eroded in the purely strength-scaling case is directly proportional to mass of the impactor and is identical for both Dactyl and Ida. Scale- or strain-rate dependence of target strength would increase the cratering efficiency and erosion rate, so that neglecting these effects should yield minimum erosion rates, i.e., lower limits valid for the situation of sand-blasting of rocky asteroid surfaces by small particles.

Gravity Scaling. Despite the fact that only a small fraction of ejecta escapes craters formed in the gravity regime, erosion can be much more efficient on soft asteroids than on their counterparts for which strength scaling is assumed to apply. The crater volume in this case is given by (Holsapple and Schmidt 1982)

$$V(D) = Ag^{-\alpha}U^{2\alpha}D^{3-\alpha}, \tag{A3}$$

where A is a constant, g is the gravitational acceleration, U is the impactor speed, and α is a scaling exponent in the range of $\frac{3}{7}$ to $\frac{3}{4}$. The fraction of ejecta exceeding the escape velocity U_{esc} depends upon the crater radius r, and can be derived from (Housen *et al.* 1983)

$$F_{esc} = k\, U_{esc}^{-e_v}\, g^{e_v/2}\, r^{e_v/2}, \tag{A4}$$

where k is a constant of order unity (see discussion by Asphaug and Nolan 1992) and

$$e_v = 6\alpha/(3 - \alpha). \tag{A5}$$

We let the crater radius r be related to the crater volume V by a coefficient B such that $V = 8Br^3$. Then

$$r = \tfrac{1}{2}(A/B)^{1/3}g^{-\alpha/3}U^{2\alpha/3}D^{(3-\alpha)/3}. \tag{A6}$$

Substituting

$$U_{esc} = \sqrt{\frac{3}{2\pi\rho G}}\, g \tag{A7}$$

and multiplying yields

$$\begin{aligned} V(D) * F_{esc}(D) &= Ak[\tfrac{1}{3}\pi\rho G(A/B)^{1/3}]^{e_v/2}U^{e_v}g^{-e_v}D^3 \\ &= (\text{constant}) * g^{-e_v}D^3 \\ &= h'D^3. \end{aligned} \tag{A8}$$

As in the strength-scaling case, the mass eroded per mass of projectile is independent of the size of the impactor. Because of the reduced gravity, however, equal-sized impactors will remove between 20 and 500 times more mass from Dactyl than from Ida, depending upon the value of e_v.

The following constants are assumed for the calculations reported in Tables II and III:

	α	e_v	k	A	B
Rubble	0.65	1.66	1.0	0.0815	.06
Sand	0.51	1.23	1.0	0.161	.06

ACKNOWLEDGMENTS

Thanks are due to Joseph Plassmann for assistance with figure preparation, to Jay Melosh, Boris Ivanov, Clark Chapman, Don Davis, and Brett Gladman for helpful discussions, and to Peter Thomas for the timely provision of a shape model for Ida. We also thank Robin Canup and Francesco Marzari for constructive comments on an earlier draft of this manuscript.

REFERENCES

Andrews, R. 1975. Origin and distribution of ejecta from near-surface laboratory- scale cratering experiments, U.S. Air Force Report AFWL-TR-74-314.

Asphaug, E., and M. Nolan 1992. Analytic and numerical predictions for regolith production on asteroids. *Proc. Lunar Planet Sci. Conf. 23rd,* 43–44. [abstract]

Asphaug, E., and H. J. Melosh 1993. The Stickney impact of Phobos: A dynamical model. *Icarus* **101,** 144–164.

Asphaug, E., J. Moore, D. Morrison, W. Benz, M. C. Nolan, and R. Sullivan 1996. Mechanical and geological effects of impact cratering on Ida. *Icarus* **120,** 158–184.

Banaszkiewicz, M., and W.-H. Ip 1991. A statistical study of impact ejecta distribution around Phobos and Deimos. *Icarus* **90,** 237–253.

Belton, M. J. S., J. Veverka, P. Thomas, P. Helfenstein, D. Simonelli, C. Chapman, M. Davies, R. Greeley, R. Greenberg, J. Head, S. Murchie, K. Klaasen, T. Johnson, A. McEwen, D. Morrison, G. Neukum, F. Fanale, C. Anger, M. Carr, and C. Pilcher 1992. Galileo Encounter with 951 Gaspra: First pictures of an asteroid. *Science* **257,** 1647–1652

Belton, M. J. S., C. R. Chapman, J. Veverka, K. P. Klaasen, A. Harch, R. Greeley, R. Greenberg, J. W. Head III, A. McEwen, D. Morrison, P. C. Thomas, M. E. Davies, M. H. Carr, G. Neukum, F. P. Fanale, D. R. Davis, C. Anger, P. J. Gierasch, A. P. Ingersoll, and C. B. Pilcher 1994. First images of 243 Ida. *Science* **265,** 1543–1547.

Belton, M. J. S., C. R. Chapman, P. C. Thomas, M. E. Davies, R. Greenberg, K. Klaasen, D. Byrnes, L. D'Amario, S. Synnott, T. V. Johnson, A. McEwen, W. Merline, J.-M. Petit, A. Storrs, J. Veverka, B. Zellner and the Galileo Imaging Team 1995. The bulk density of asteroid 243 Ida from Dactyl's orbit. *Nature* **374,** 785–788.

Belton, M. J. S., C. R. Chapman, K. P. Klaasen, A. Harch, P. C. Thomas, J. Veverka, A. McEwen, and R. Pappalardo 1996. Galileo's encounter with 243 Ida: An overview of the imaging experiment. *Icarus* **120,** 1–19.

Binzel, R., S. M. Slivan, P. Magnusson, W. Z. Wisniewski, J. Drummond, K. Lumme, M. A. Barucci, E. Dotto, C. Angeli, D. Lazarro, S. Mottola, M. Gonano-Beurer, T. Michałowski, G. De Angelis, D. J. Tholen, M. Di Martino, M. Hoffmann, E. H. Geyer, and F. Velichko 1993. Asteroid 243 Ida: Groundbased photometry and a pre-Galileo physical model. *Icarus* **105,** 310–325.

Bottke, W., M. Nolan, R. Greenberg, and R. Kolvoord 1994. Velocity distributions among colliding asteroids. *Icarus* **107,** 255–268.

BURNS, J. 1986. Some background about satellites. *Satellites* (J. Burns and M. Matthews, Eds.), pp. 1–38. Univ. of Arizona Press, Tucson.

CARR, M., R. KIRK, A. MCEWEN, J. VEVERKA, P. THOMAS, J. HEAD, AND S. MURCHIE 1994. The geology of Gaspra. *Icarus* **107,** 61–71.

CHAPMAN, C. R., W. MERLINE, D. DAVIS, J. VEVERKA, M. J. S. BELTON, T. V. JOHNSON, AND THE GALILEO IMAGING TEAM 1994. Ida's satellite: Its origin and impact history. *Bull. Am. Astron. Soc.* **26,** 1157. [abstract]

DAVIS, D., K. HOUSEN, AND R. GREENBERG 1981. The unusual dynamical environment of Phobos and Deimos. *Icarus* **47,** 220–233.

DAVIS, D. R., C. CHAPMAN, D. DURDA, P. FARINELLA, AND F. MARZARI 1996. The formation and collisional/dynamical evolution of the Ida/Dactyl system as part of the Koronis family. *Icarus* **120,** 220–230.

DOBROVOLSKIS, A., AND J. BURNS 1980. Life near the Roche limit: Behavior of ejecta from satellites close to planets. *Icarus* **42,** 422–441.

DOHNANYI, J. 1969. Collisional model of asteroids and their debris. *J. Geophys. Res.* **74,** 2531.

DURDA, D. 1996. The formation of asteroidal satellites in catastrophic collisions. *Icarus* **120,** 212–219.

FARINELLA, P., AND D. DAVIS 1994. Will the real asteroid size distribution please step forward. *Proc. Lunar Planet. Sci. Conf. 25th,* 365–366. [abstract]

GEISSLER, P., J.-M. PETIT, AND R. GREENBERG 1995a. Ejecta reaccretion on rapidly rotating asteroids: Implications for 243 Ida and 433 Eros. *Proc. Astron. Soc. Pac.,* submitted.

GEISSLER, P., J.-M. PETIT, AND R. GREENBERG 1995b. Ejecta reaccretion on rapidly rotating asteroids: Implications for 243 Ida and 433 Eros. *Proc. Lunar. Planet. Sci. Conf. 26th,* 449–450. [abstract]

GREENBERG, R., M. NOLAN, W. BOTTKE, R. KOLVOORD, AND J. VEVERKA 1994. Collisional history of Gaspra. *Icarus* **107,** 84–97.

HOLSAPPLE, K. 1993. The scaling of impact processes in planetary sciences. *Annu. Rev. Earth Planet. Sci.* **21,** 333–373.

HOLSAPPLE, K. AND R. SCHMIDT 1982. On the scaling of crater dimensions. 2. Impact processes. *J. Geophys. Res.* **87**(B3), 1849–1870

HOUSEN, K. R., R. M. SCHMIDT, AND K. A. HOLSAPPLE 1983. Crater ejecta scaling laws: Fundamental forms based on dimensional analysis. *J. Geophys. Res.* **88,** 2485–2499.

HOUSEN, K. R., R. M. SCHMIDT, AND K. A. HOLSAPPLE 1991. Laboratory simulations of large scale fragmentation events. *Icarus* **94,** 180–190.

KELLOGG, O. D. 1929. *Foundations of potential theory*. Ungar, New York.

LAGERKVIST, C.-I., A. HARRIS, AND V. ZAPPALÀ 1989. Asteroid lightcurve parameters. In *Asteroids II* (R. Binzel, T. Gehrels and M. Matthews, Eds.). Univ. of Arizona Press, Tucson.

LEE, P., J. VEVERKA, P. THOMAS, P. HELFENSTEIN, M. J. S. BELTON, C. CHAPMAN, R. GREELEY, R. PAPPALARDO, R. SULLIVAN, AND J. W. HEAD III 1996. Ejecta blocks on 243 Ida and on other asteroids. *Icarus* **120,** 87–105.

LEE, S. W., P. THOMAS, AND J. VEVERKA 1986. Phobos, Deimos and the Moon: Size and distribution of crater ejecta blocks. *Icarus* **68,** 77–86.

MARZARI, F., D. DAVIS, AND V. VANZANI 1995. Collisional evolution of asteroid families. *Icarus* **113,** 168–187.

MELOSH, H. J. 1989. *Impact Cratering, a Geologic Process*. Oxford Univ. Press, Oxford.

MOORE, H. 1972. Ranger and other impact craters photographed by Apollo 16. Apollo 16 Preliminary Science Report NASA SP-315, pp. 29–45 to 29–51.

NOLAN, M. C., E. ASPHAUG, H. J. MELOSH, AND R. GREENBERG 1995. Impact craters of asteroids: Does gravity or strength control their size? *Icarus,* submitted.

SOTER, S. 1971. The dust belts of Mars. Cornell Center for Radiophysics and Space Research Report 462.

SULLIVAN, R., R. GREELEY, R. PAPPALARDO, E. ASPHAUG, J. M. MOORE, D. MORRISON, M. J. S. BELTON, M. CARR, C. R. CHAPMAN, P. GEISSLER, R. GREENBERG, JAMES GRANAHAN, J. W. HEAD III, R. KIRK, A. MCEWEN, P. LEE, P. C. THOMAS, AND J. VEVERKA 1996. Geology of 243 Ida. *Icarus* **120,** 119–139.

THOMAS, P. 1979. Surface features of Phobos and Deimos. *Icarus* **40,** 223–243.

THOMAS, P., M. J. S. BELTON, B. CARCICH, C. R. CHAPMAN, M. E. DAVIES, R. SULLIVAN, AND J. VEVERKA 1996. The shape of Ida. *Icarus* **120,** 20–32.

VAN HOUTEN, C., I. VAN HOUTEN-GROENEVELD, P. HERGET, AND T. GEHRELS 1970. The Palomar–Leiden survey of faint minor planets. *Astron. Astrophys.* Suppl. 2, p. 339.

VEVERKA, J., AND P. THOMAS 1979. Phobos and Deimos: A preview of what asteroids are like. In *Asteroids* (T. Gehrels, Ed.) pp. 628–654. University of Arizona Press, Tucson.

VEVERKA, J., P. THOMAS, P. LEE, P. HELFENSTEIN, M. J. S. BELTON, C. CHAPMAN, K. KLAASEN, T. V. JOHNSON, A. HARCH, M. DAVIES, AND THE GALILEO IMAGING TEAM 1994. Ida's satellite: what is it like? *Bull. Am. Astron. Soc.* **26,** 1155. [Abstract]

VEVERKA, J., P. HELFENSTEIN, P. LEE, P. THOMAS, A. MCEWEN, M. BELTON, K. KLAASEN, T. V. JOHNSON, J. GRANAHAN, F. FANALE, P. GEISSLER, AND J. W. HEAD 1996a. Ida and Dactyl: Spectral reflectance and color variations. *Icarus* **120,** 66–76.

VEVERKA, J., P. THOMAS, P. HELFENSTEIN, P. LEE, A. HARCH, S. CALVO, C. CHAPMAN, M. J. S. BELTON, K. KLAASEN, T. V. JOHNSON, AND M. DAVIES 1996b. Dactyl: Galileo observations of Ida's satellite. *Icarus* **120,** 200–211.